

1 Characterization of a commercial lower-cost medium precision NDIR sensor for atmospheric CO₂
2 monitoring in urban areas.

3
4 Emmanuel Arzoumanian¹, Felix R. Vogel^{2*}, Ana Bastos¹, Bakhram Gaynullin³, Olivier Laurent¹,
5 Michel Ramonet¹ and Philippe Ciais^{1*}

6
7 1 LSCE/IPSL, CEA-CNRS-UVSQ, Université Paris-Saclay, Gif-Sur-Yvette, France

8 2 Climate Research Division, Environment and Climate Change Canada, Toronto, Canada

9 3 SenseAir AB, Delsbo, Sweden

10
11 * Corresponding authors: Felix.Vogel@canada.ca and Philippe.Ciais@lsce.ipsl.fr

12 **Abstract:**

13
14 CO₂ emission estimates from urban areas can be obtained with a network of in-situ instruments
15 measuring atmospheric CO₂ combined with high-resolution (inverse) transport modeling. Because
16 the distribution of CO₂ emissions is highly heterogeneous in space and variable in time in urban
17 areas, gradients of atmospheric CO₂ (here, dry air mole fractions) need to be measured by
18 numerous instruments placed at multiple locations around and possibly within these urban areas.
19 This calls for the development of lower-cost medium precision sensors to allow a deployment at
20 required densities. Medium precision is here set to be a random error (uncertainty) on hourly
21 measurements of ± 1 ppm or less, a precision requirement based on previous studies of network
22 design in urban areas. Here we present tests of newly developed NDIR sensors manufactured by
23 Senseair AB performed in the laboratory and at actual field stations, the latter for CO₂ dry air mole
24 fractions in the Paris area. The lower-cost medium precision sensors are shown to be sensitive to
25 atmospheric pressure and temperature conditions. The sensors respond linearly to CO₂ when
26 measuring calibration tanks, but the regression slope between measured and assigned CO₂ differs
27 between individual sensors and changes with time. In addition to pressure and temperature
28 variations, humidity impacts the measurement of CO₂, all of these factors resulting in systematic
29 errors. In the field, an empirical calibration strategy is proposed based on parallel measurements
30 with the lower-cost medium precision sensors and a high-precision instrument cavity ring-down
31 instrument during 6 months. The empirical calibration method consists of using a multivariable
32 regression approach, based on predictors of air temperature, pressure and humidity. This error
33 model shows good performances to explain the observed drifts of the lower-cost medium precision
34 sensors on time scales of up to 1-2 months when trained against 1-2 weeks of high-precision
35 instrument time series. Residual errors are contained within the ± 1 ppm target, showing the
36 feasibility to use networks of HPP3 instruments for urban CO₂ networks. Provided that they could
37 be regularly calibrated against one anchor reference high-precision instrument these sensors
38 could thus collect the CO₂ (dry air) mole fraction data required as for top-down CO₂ flux estimates.

39 40 **1. Introduction**

41
42 Urban areas cover only a small portion (< 3 %) of the land surface but account for about 70% of
43 fossil fuel CO₂ emissions (Liu et al. 2014, Seto et al. 2014). Uncertainties of fossil fuel CO₂
44 emissions from inventories based on statistics of fuel amounts and/or energy consumption are on
45 the order of 5% for OECD countries and up to 20% in other countries (Andres et al. 2014) but they
46 are larger in the case of cities (Breon et al. 2015, Wu et al. 2016). Further, in many cities of the
47 world, there are no emission inventories available. The need for more reliable information on
48 emissions and emission trends has prompted research projects seeking to provide estimates of

49 GHG budget cities, power plants and industrial sites. These are often based on in situ
50 measurements made at surface stations (Staufer et al. 2016, Lauvaux et al. 2016, Verhulst et al.
51 2017), aircraft campaigns around emitting locations (Mays et al. 2009, Cambaliza et al. 2014) and
52 satellite imagery (Broquet et al. 2017, Nassar et al. 2017). Although sampling strategies and
53 measurement accuracies differ between these approaches, the commonly used principle is to
54 measure atmospheric CO₂ dry air mole fraction gradients at stations between the upwind and
55 downwind vicinity of an emitting area and infer the emissions that are consistent with those CO₂
56 gradients and their uncertainties, using an atmospheric transport model. This approach is known
57 as atmospheric CO₂ inversion or as a “top-down” estimate.

58 Inversion studies from Paris, France attempting to constrain CO₂ emissions from measurements
59 of CO₂ dry air mole fractions at stations located around the city along the dominant wind direction,
60 have pointed out that the fast mixing by the atmosphere and the complex structure of urban CO₂
61 emissions requires high resolution atmospheric transport models, and continuous measurements
62 of the atmosphere to select gradients induced by emission plumes (Broquet et al. 2015, Wu et al.
63 2016) that can be captured at the scale of the model.

64 With the existing three stations, the CO₂ emissions from the Paris megacity could be retrieved
65 with an accuracy of ≈20% on monthly budgets (Staufer et al. 2016). A denser network of stations
66 would help to obtain more information on the spatial details of CO₂ emissions. A network design
67 study by Wu et al. 2016 for the retrieval of CO₂ emissions per sector for the Paris Megacity has
68 shown that with 10 stations measuring CO₂ with 1 ppm accuracy on hourly time-steps, the error
69 of the annual emission budget could be reduced down to a 10% uncertainty. Wu et al. 2016
70 furthermore found that for a more detailed separation of emissions into different sectors, more
71 stations were needed, on the order of 70 stations to be able to separate road transport from
72 residential CO₂ emissions. This inversion based on pseudo-data allowed estimating total CO₂
73 emissions with a better accuracy than 10% and emissions of most major source sectors (building,
74 road energy) with an accuracy better than 20%. Another urban network design study over the San
75 Francisco Bay area reached a similar conclusion, i.e. that in-situ CO₂ measurements from 34
76 stations with 1 ppm accuracy at an hourly resolution could estimate weekly CO₂ emissions from
77 the city area with less than 5 % error (Turner et al. 2016).

78 In the studies from Wu et al. 2016 and Turner et al. 2016, the additional number of atmospheric
79 CO₂ measurement stations rather than the individual accuracy of each measurement helped to
80 constrain emissions, provided that CO₂ observation errors have random errors of less than 1 ppm
81 on hourly measurements, uncorrelated in time and in space between stations. Therefore, we will
82 adopt here a 1 ppm uncertainty on hourly CO₂ data as the target performance for new urban lower-
83 cost medium precision CO₂ sensors.

84 Today, the continuous CO₂ gas analyzers used for continental scale observing systems like ICOS
85 (<https://www.icos-ri.eu/>), NOAA (<https://www.esrl.noaa.gov/gmd/>) or ECCO
86 (<https://www.canada.ca/en/environment-climate-change.html>) follow the WMO/GAW guidelines
87 and are at least ten times more precise than our target of 1 ppm, but are also quite expensive. For
88 urban inversion-based flux estimates for Paris, Wu et al. 2016 found that the number of
89 instruments is more important than their individual precision. Furthermore, Turner et al. (2016)
90 reported that weekly urban CO₂ fluxes in the Bay Area (California, USA) can be estimated at a
91 precision of 5% when deploying a dense network of sensors (ca. every 2km) with an assumed
92 mismatch error of 1ppm. This underlines that significant expansion of urban networks is desirable
93 and could be achieved at an acceptable cost if low-cost sensors could be produced with the
94 specifications of 1 ppm random error (i.e. bias free long-term repeatability). .

95 Recently, inexpensive sensors, measuring trace gases, particulate matter, as well as traditional
96 meteorological variables, using various technologies and accuracy have become commercially
97 available. Evaluation and implementation of these sensors is quite promising (Eugster and Kling
98 2012, Holstius et al. 2014, Piedrahita et al. 2014, Young et al. 2014, Wang et al. 2015). With the
99 advent of low cost mid-IR light sources and detectors, different non-dispersive infrared (NDIR)

100 CO₂ sensors have become commercially available and were tested for their suitability for CO₂
101 monitoring (e.g. Martin et al. 2017, Kunz et al. 2017) or for CO₂ in combination with air pollutants
102 (e.g. Shusterman et al. 2016, Zimmerman et al. 2018).
103 In this study, we present the development and stability tests of a low-cost sensor (HPP3, SenseAir
104 AB, Sweden) to measure the mole fraction of CO₂ of ambient air (Hummelgard et al. 2015).
105 Throughout the manuscript we will use {CO₂} to signify the mole fraction and/or dry air mole
106 fraction of CO₂ in air. To improve performance and eventually derive dry air mole fractions,
107 additional parameters are measured in ambient air and the sensor is integrated into a platform,
108 which we will refer to as instrument. Then, the instrument linearity is evaluated against a suite of
109 CO₂ reference gases with CO₂ dry air mole fractions from 330 to 1000 ppm. The instrument's
110 sensitivities to ambient air temperature, pressure and water vapor content are assessed in
111 laboratory experiments and climate chambers tests. The calibrated low-cost medium precision
112 (LCMP) instruments are then compared to highly precise CRDS instruments (G2401, Picarro Inc,
113 Santa Clara, USA).
114 Lastly, we present the time series of ambient air CO₂ measurements in the Paris region. The time
115 series are compared to measurements by co-located cavity ring down spectroscopy (CRDS)
116 analyzers, and an empirical corrections and calibration scheme to the HPP3-based instrument are
117 proposed based on measured CO₂ dry mole air fractions and meteorological variables. These
118 corrections and calibrations are established during a period of 1 or 2 weeks are used to estimate
119 the drift of the HPP3-instrument on time scales of up to a month and a half.

120

121 **2. Sensor integration**

122

123 **2.1. HPP3 sensor**

124

125 The HPP (High-Performance Platform) NDIR (Non-Dispersive InfraRed) CO₂ sensor from
126 SenseAir AB (Delsbo, Sweden) is a commercially available lower-cost system (Hummelgard et al.
127 2015). The main components of this sensor are an infrared source (lamp), a sample chamber (ca.
128 1 m optical path length), a light filter and an infrared detector. The gas in the sample chamber
129 causes absorption of specific wavelengths (Hummelgard et al. 2015) according to the Beer–
130 Lambert law, and the attenuation of light at these wavelengths is measured by a detector to
131 determine the gas mole fraction. The detector has an optical filter in front of it that eliminates all
132 light except the wavelength that the selected gas molecules can absorb. The HPP has a factory
133 pre-calibrated CO₂ measurement range of 0 to 1000 ppm. The HPP sensor itself uses ca. 0.6 W
134 and requires an operating voltage of 12 V direct current and has a life expectancy superior to 15
135 years according to the manufacturer.

136 Three generation of HPP sensors were built by SenseAir AB (Delsbo, Sweden). In this manuscript
137 we only report on the tests carried out on the latest generation (HPP3) being the most performant
138 among the HPP sensors family. Previous HPP generations were used for more short-term
139 airborne measurements, for example in the COCAP system (Kunz et al. 2017) and were found to
140 have an accuracy of 1-1.2 ppm during short-term mobile campaigns. A number of technical
141 improvements have been made for the new HPP3 generation described here:

- 142 • Simple interface through USB connection and the development of a new software made
143 data transfer easier, quicker and more efficient
- 144 • Improved temperature stability due to 6 independent heaters dispatched inside the unit.
- 145 • To reduce long-term drift the sensor is equipped with new electronics and the IR sources
146 were preconditioned prior to shipment.
- 147 • The improved second version of HPP3 (HPP3.2) sensors was equipped with a pressure
148 sensor (LPS331AP - ST Microelectronics, Switzerland) to allow real-time corrections. The
149 high resolution mode of the LPS331AP has a pressure range of 263 to 1277 hPa and a

150 Root Mean Square (RMS) of 0.02 hPa can be achieved with a low power consumption (i.e.
151 30 μ A).

- 152 • The impact of leaks on the measurements are reduced since the third generation sensor
153 works in a high pressure mode. A pump is thus needed upstream of the sensor inlet in
154 order to create a high pressure in the measurement cell.

155
156 Different sensors from two versions of HPP were tested and used in this study, that is, three
157 sensors from a first version (HPP3.1) named S1.1, S1.2 and S1.3, and three others from the
158 second version (HPP3.2) named S2.1, S2.2 and S2.3. For the HPP3.1 sensors, an internal
159 pressure compensation does not exist, but the HPP3.2 series includes a pressure sensor together
160 with a compensation algorithm, which normalizes measured CO₂ dry air mole fractions according
161 to ambient pressure (Gaynullin et al. 2016).

162

163 **2.2. Portable integrated instrument**

164

165 The HPP3 sensors were integrated into a custom-built portable unit, which we will refer to as
166 instrument. This instrument should be suitable to perform in-situ CO₂ measurements on ambient
167 air. The instrument is composed of the HPP3 CO₂ sensor, temperature (T) and relative humidity
168 (RH) sensors. To be able to continuously flush the measurement cell a diaphragm micro pump
169 with a built-in potentiometer (GardnerDenverThomas, USA, Model 1410VD/1.5/E/BLDC/12V) was
170 added upstream of the HPP3's optical cell. Temperature and RH were measured at the exterior
171 of the optical cell where gas is released into the surrounding enclosure. For these humidity and
172 temperature, a DHT22 sensor kit (Adafruit, USA) was added and connected through an I2C
173 interface. The accuracy of the sensor is $\pm 2-5\%$ RH and $\pm 0.5^\circ\text{C}$. Its range is 0-100 %RH and -40
174 to $+80^\circ\text{C}$, respectively. The response time for all sensors was less than one minute (which is the
175 time-step to which data was integrated).

176 A Raspberry Pi3 (RPi3) (Raspberry Pi Foundation, 2015) is used to collect the data of all sensors.
177 The RPi3 is a small (85x56 mm²) single-board computer running Rasbian OS, an open-source
178 GNU/Linux distribution. The HPP3 sensors were connected via USB. A 7" touch screen monitor is
179 connected via an adapter board which handles power and signal conversion. The package is
180 powered by a switching power supply providing 12V, but can also be run on a 12V battery pack.
181 An image of the components of the portable instrument package is available in Figure 1.

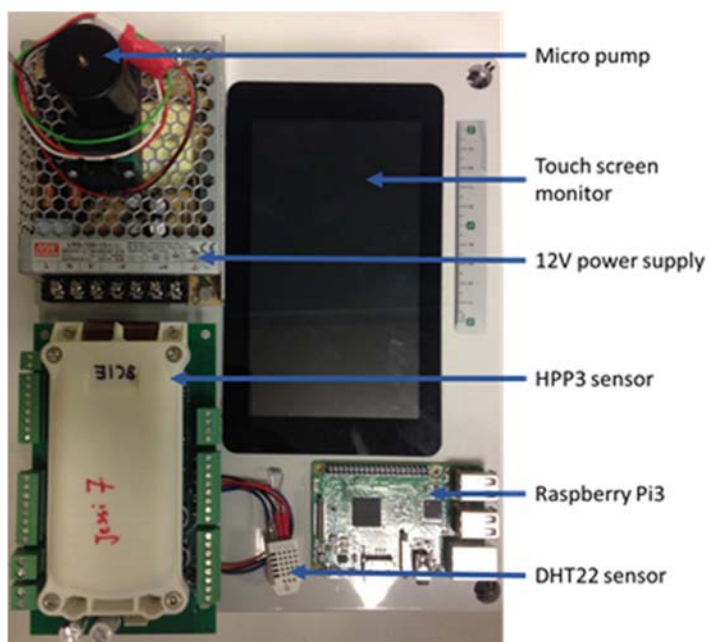


Figure 1: Components of the portable instrument on the top of its box.

182
183
184
185
186
187
188
189
190
191
192
193
194
195
196
197
198
199

3. Methods

NDIR sensors are sensitive to IR light absorption by CO₂ molecules in the air contained in their optical cell, but the retrieval of CO₂ dry air mole fraction to the desired uncertainty of 1 ppm is made difficult by sensitivities to temperature, pressure and humidity. Therefore, these parameters should be controlled as much as possible, and their sensitivities characterized, to correct and calibrate reported {CO₂}. A series of tests were carried out to characterize the HPP3.1 (S1.1, S1.2, S1.3) and HPP3.2 (S2.1, S2.2, S2.3) performances and sensitivities to {CO₂}, T, p and RH. Firstly, temperature, pressure and {CO₂} sensitivities were determined in laboratory experiments. Then, field measurements were conducted with an accurate CRDS instrument (Picarro, USA, G2401) measuring the same air as the HPP3 sensors. The CRDS short-term repeatability is estimated to be below 0.02 ppm and the long-term repeatability to be below 0.03 ppm (Yver-Kwok et al. 2015). Table 1 summarizes all laboratory tests and field test measurements, which are presented in this section.

Name	Purpose	Location	Air measured	Parameter	Range of T (°C), and p (hPa)	Range of [CO ₂] in ambient air (ppm)	Range of [CO ₂] in Cal. Cylinders (ppm)	Duration (days)	Sensors tested
PT1	Correlation between [CO ₂] and P,T	Laboratory (Saclay)	Calibration cylinders	T, p	16 to 32 and 968.7 to 1038.6	N/A	420 to 450	3	S1.1, S1.2, S1.3
PT2	Correlation between [CO ₂] and P,T	PIT climate chamber (Guyancourt)	Calibration cylinders	T, p	-2 to 35 and 759.9 to 1013.3	N/A	420 to 450	5	S2.1, S2.2, S2.3
DA1	Test calibration frequency	Laboratory (Saclay)	Calibration cylinders and	T, p, RH, {CO ₂ } from CRDS	24 to 31 and	417 to 575	330 to 1000	48	S1.1, S1.2, S1.3

			dried ambient air		1009.2 to 1023.4				
WA2-1	Test calibration frequency	Field station (Saclay)	Ambient air	T, p, RH, {CO ₂ } from CRDS	25 to 27 and 1012.2 to 1021.4	389 to 508	N/A	45	S2.2, S2.3
WA2-2	Test calibration frequency	Field station (Jussieu)	Ambient air	T, p, RH, {CO ₂ } from CRDS	29 to 31 and 0.993 to 1034.5	393 to 521	N/A	60	S2.1

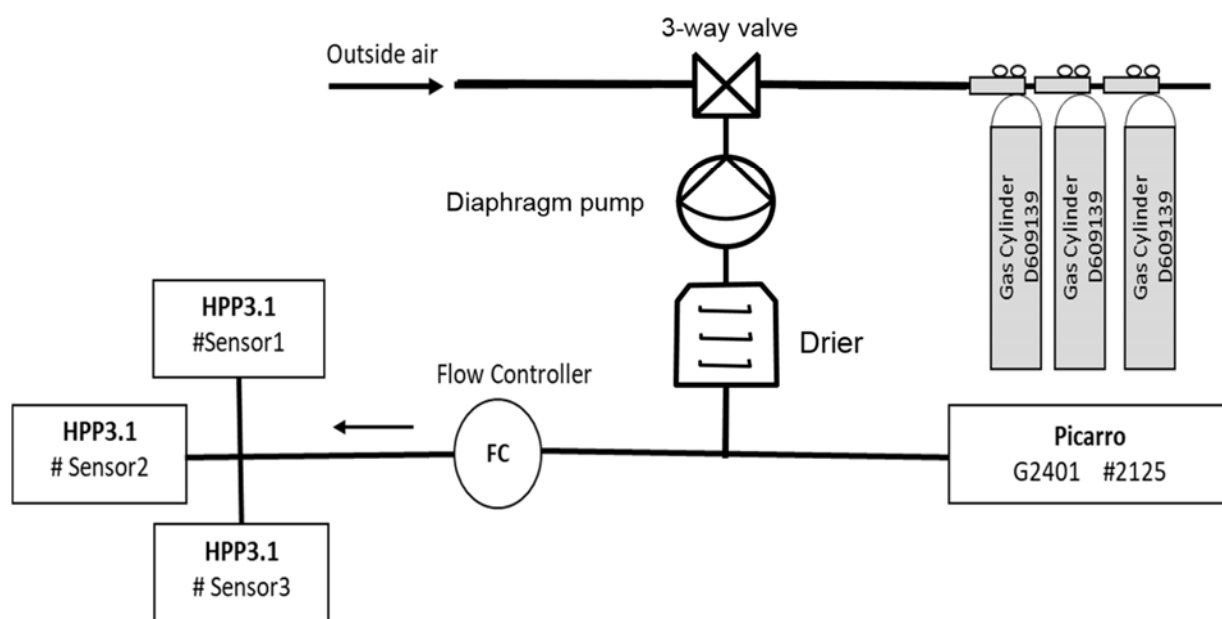
200 **Table 1:** Summary of all laboratory tests.

201

202 **3.1. Laboratory tests**

203

204 All laboratory tests used the same fundamental setup shown in Figure 2 with only slight
 205 modifications. A diaphragm pump (KNF Lab, Germany, Model N86KN.18) was used to pump air
 206 from either an ambient air line or calibration cylinders to a Nafion dryer (PermaPure, USA, MD-
 207 070 series) was used to eliminate H₂O traces in the gas line. A flow controller (Bronkhorst, France,
 208 EI-Flow series) was used to regulate the airflow distributed with a manifold to the HPP3
 209 instruments at 500 mL min⁻¹ to ensure stable experimental conditions while a CRDS instrument
 210 could also be connected through a gas split to measure the same air.



211

212

213 **Figure 2:** Test setup

214

215 **3.1.1. Sensitivity to temperature and pressure variations**

216

217 To assess the linearity of the response of each sensor to {CO₂} for different pressure and
 218 temperature conditions, two series of temperature and pressure sensitivity tests (PT1, PT2) were
 219 realized in a closed chamber with controlled T and p for the HPP3.1 and HPP3.2 sensors No drier
 220 was necessary as dried air from high-pressure cylinders was used. The CRDS instrument (Picarro,
 221 G2401, serial number 2125) was not connected during these tests

222 In test PT1 (table1), three HPP3.1 sensors were put in a simple plastic chamber and exposed to
223 pressure changes ranging from 977.8 to 1038.6 hPa, and temperature ranges of 16 to 32 °C, while
224 measuring gas from a calibration cylinder. Pressure and temperature were measured by a high-
225 precision pressure sensor (Keller, Germany, Series 33x, 0.2hPa and 0.05K precision).

226 In test PT2, to test wider ranges for pressure and temperature, that might be experienced during
227 field measurements, three HPP3.2 sensors were placed inside a dedicated temperatures and
228 pressure chamber at the Plateforme d'Integration et de Tests (PIT) at OVSQ Guyancourt, France
229 where a much larger range of T and p variations could be applied. During each T, p test, four
230 calibration cylinders with dry air CO₂ dry air mole fractions from 420 to 450 ppm were measured
231 by all the HPP3.2 sensors for a period of approximately 120 hours for each cylinder. In the PIT
232 chamber, temperature was varied from -2 to 35 °C with a constant rate of change of 1 °C/h keeping
233 pressure constant at a value of 1013.25 hPa. During pressure tests the chamber pressure was
234 varied from 1013.25 to 759.94 hPa with a decrement of 50.66 hPa, being regulated with a primary
235 pump, with temperature fixed at 15°C.

236

237 **3.1.2. Correction and calibration of CO₂ measurements for dry and wet air**

238

239 These experiments were performed to evaluate the response of HPP3 sensors to {CO₂} changes
240 in ambient air. Corrections were established to allow compensating for unintended instrument
241 behavior and sensitivities, while calibrations are applied to translate the instruments readings to
242 the WMO/GAW CO₂ scale (here, XCO₂ 2007). Both steps are combined into one procedure. Two
243 modes of operation for the HPP3 sensors have been tested i.e. using a dried or an undried gas
244 stream, as those are two common modes of operation in greenhouse gas measurements in
245 different local, regional and global networks (GAW report 242).

246

247 **Dry air experiments**

248

249 Water vapor is known to interfere with CO₂ measurements, in particular for NDIR sensors. It is
250 thus important to determine the response of the sensors to {CO₂} under the best possible
251 conditions, that is, dry air. The experimental setup shown in Figure 2 was used. In test DA1 (Table
252 2) different HPP3 sensors were flushed with the same dry ambient air, passed through a Nafion
253 dryer. CRDS measurement were used to monitor and confirm that H₂O was reduced to trace
254 amounts, i.e. 0.05 ±0.05 % H₂O. HPP3.1 sensors S1.1, S1.2, S1.3 were tested extensively during
255 45 days, and HPP3.2 sensors S2.1, S2.2 were tested during 12 days.

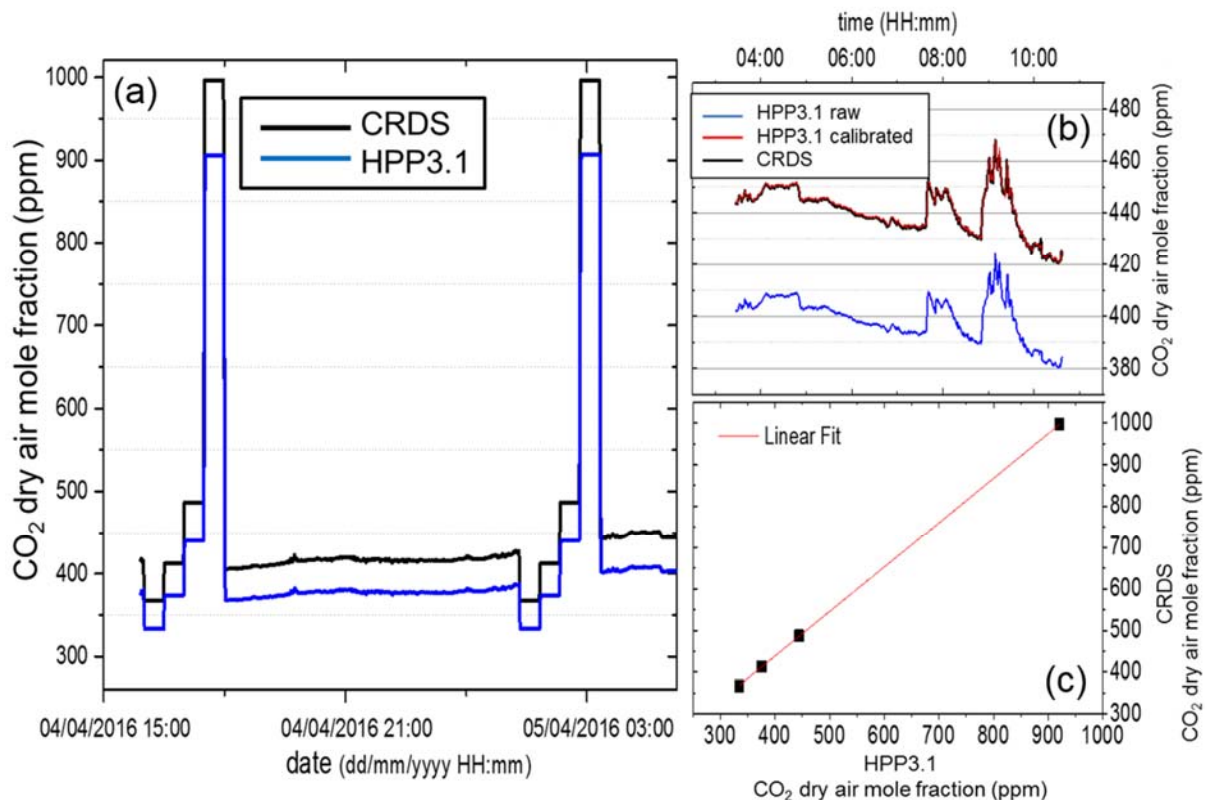
256 Additionally, for a period of 45 days during spring 2016, S1.1, S1.2 and S1.3 measurements of
257 dry ambient air in parallel with a co-deployed CRDS instrument (Picarro, USA, G2401) were
258 conducted at the Saclay field site (see section 3.3.1) There ambient air was pumped from a
259 sampling line fixed on the roof of the building (ca. 4 m above ground level) to flush the setup
260 described in Fig. 2. Four dry-air calibration cylinders (330 ppm, 375 ppm, 445 ppm and 1000 ppm
261 of {CO₂}) were measured once every 13 hours they were sampled successively each for 30
262 minutes (Figure 3). As the HPP3 responses can be slow and in order to remove memory effects,
263 only the last 15 minutes of each measurement period were used.

264

265 **Undried (wet) air experiments**

266

267 As drying is impractical for some applications, we also measured the HPP3's sensitivities to water
268 vapor in undried ambient air and calibration cylinders. If these sensitivities were stable over time,
269 they could be used to correct reported {CO₂} for the H₂O interference. For WA2-1 and WA2-2
270 tests, the Nafion dryer was removed from the setup. The only modification of the experiment was
271 the removal of the Nafion drier.



272
 273 **Figure 3:** (a) CO₂ dry air mole fractions measured by S1.1 (blue) and the Picarro CRDS analyzer
 274 (black). (b) Calibrated dry air mole fractions of S1.1 (red) compared to the raw values (blue).
 275 (c) Four reference gases (assigned values are 367 ppm, 413 ppm, 487 ppm and 997 ppm of
 276 {CO₂}), are used for the calibration. No saturation effects are observed within our CO₂ dry air mole
 277 fraction range.

278
 279 **3.2. Instrument correction and calibration procedure**
 280
 281 In order to correct the reported {CO₂} we have to define a function that allows to correct for
 282 unintended instrument sensitivities i.e. to p, T, H₂O as well as to correct {CO₂} measurements to
 283 an official scale should they show any offset or non-linear behavior.

284
 285 **Linearity of instrument response**
 286
 287 For dry air measurements in test DA1, a linear calibration curve was found to be appropriate. panel
 288 C of Figure 3 shows that the response of the HPP3 instruments to CO₂ dry air mole fraction is
 289 linear ($R^2 = 0.95$) from 330 to 1000 ppm. No saturation effects are observed within this CO₂ dry
 290 air mole fraction range since residuals are included in the ± 1 ppm range. Therefore, a linear
 291 response to {CO₂} is assumed further on.

292
 293 **Multivariable correction and calibration**

294 Due to the high correlation of air temperature and water vapor content, which were both found to
 295 be linear (see section 4), we suggest a multivariable regression method, which includes pressure,

296 temperature and humidity. Indeed, if variables are corrected one at a time, an overcorrection of
297 one of the correlated variables may occur.
298 Multivariable regression is a generalization of linear regression by considering more than one
299 variable. We used a multivariable linear regression of the form:

$$300 \{CO_2\}_{calibrated, corrected} = b + a_{CO_2}\{CO_2\}_{HPP3} + a_p p + a_T T + a_W W + a_d d \quad (1)$$

302 $\{CO_2\}_{calibrated, corrected}$ corresponds to the measured $\{CO_2\}$ by the reference instrument (CRDS)
303 calibrated on the WMO CO₂ X2007 scale. C is the $\{CO_2\}_{HPP3}$ reported by the HPP3 instrument,
304 with additional factors to capture the influence of the pressure p , the temperature T , the water
305 mixing ratio W (as calculated from our T , p and RH measurements), the baseline drift d and a
306 baseline offset b . All instrument specific coefficients for the multivariable linear regression are
307 determined using measurements of the parameters during several days.
308

309

310 **3.3. Field tests with urban air measurements**

311

312 To assess their real-world performance, we conducted additional tests for the HPP3 sensors
313 measuring ambient air at two field sites under typical conditions for urban air monitoring. After the
314 sensors were fully integrated into instruments as described in section 2.2. Three HPP3.1
315 instruments (S1.1, S1.2, S1.3) and two HPP3.2 instruments (S2.2, S2.3) were installed Saclay
316 field site (48.7120N, 2.1462E) to measure ambient air on top of the building roof. Saclay is located
317 20 kilometers south of the center of Paris in a low-urbanized area. In addition, one HPP3.2
318 instrument (S2.1) was installed to measure air at the Jussieu field site on the Jussieu University
319 campus in the center of Paris (48.8464N, 2.3566E).

320

321 **3.3.1. Saclay field Site tests**

322

323 The sampling line, a 5 meter Dekabon tube with an inner tube diameter of 0.6 cm, was fixed on
324 the rooftop of the building at about 4 meters above the ground, which was connected to a setup
325 that was a copy of the laboratory tests. However, up to five HPP3 instruments were connected
326 and a pump of the same built as in the previous experiments was used to regulate the air-flow
327 distributed with a manifold to the HPP3 instruments at 500 mL min⁻¹ to ensure stable experimental
328 conditions. The field site is equipped with a cooling/heating unit that was turned off most of the
329 time so that room temperature varied between 24 and 31 °C. During the test of HPP3.2 were
330 tested for 45 days. Four reference gas cylinders (330ppm, 375ppm, 445ppm and 1000 ppm of
331 CO₂) were used and each HPP3 was flushed every 12 hours for 30 minutes per cylinder during
332 the dry air experiment. No calibration cylinders were used during the undried air experiment, since
333 the calibration was based on the co-located high precision measurement with the CRDS analyzer.
334 The mean dry air mole fraction of ambient CO₂ was 420 ppm and varied between 388 ppm and
335 575 ppm during dry air experiments and a mean of 409 ppm and variations between 389 ppm and
336 509 ppm were found during the undried air experiments.

337

338 **3.3.2. Jussieu field site tests**

339 The measurements were conducted at the OCAPI (Observatoire de la Composition de l'Air de
340 Paris a l'IPSL) field station. The measurements from the HPP3.2 instrument (S2.1) in Jussieu
341 were compared with those of a co-located CRDS analyzer (Picarro, USA, G2401). Two
342 independent sampling lines (about 5 meter Dekabon tube with an inner tube of 0.6 cm) were used
343 for the CRDS and the S2.1 instrument. The air-flow into S2.1 was regulated by the micro pump
344 (see section 2.2) and set to 500 mL min⁻¹ using a potentiometer. At this location neither calibration

345 cylinders nor a drying system were deployed for S2.1, but used to calibrate the CRDS. The
346 measurement period was 60 days and the mean ambient CO₂ dry air mole fraction was 410 ppm
347 and minute averages varied between 393 ppm and 521 ppm. Room temperature varied between
348 28 and 31 °C during the observation period.

349

350 **4. Results**

351

352 **4.1. Sensitivity to temperature and pressure variations using dried air**

353

354 **4.1.1. HPP3.1 instruments tested in the simple chamber (PT1)**

355

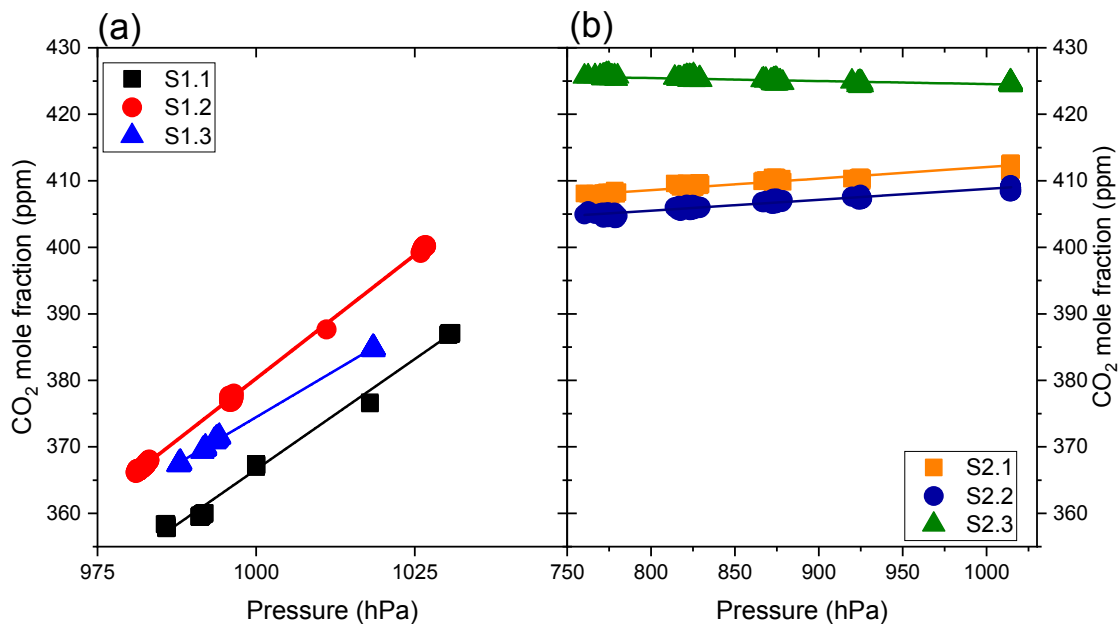
356 Linear relationships are observed between reported CO₂ dry air mole fractions and p, T ($R^2 = 0.99$
357 with p and $R^2 = 0.92$ with T) in the simple chamber (see Figure 4 and 5). Due to the limitation of
358 experimental conditions in these simple plastic chambers, only a narrow pressure range of 977.78
359 to 1033.52 hPa and a temperature range of 16 °C to 32 °C could be tested for these instruments.
360 Different slopes and intercepts are found for each instrument as reported in Table 2. This indicates
361 that there is no single universal p and T calibration curve that could be determined for one
362 instrument and used for others.

363

364 **4.1.2. HPP3.2 instruments tested in the PIT chamber (PT2)**

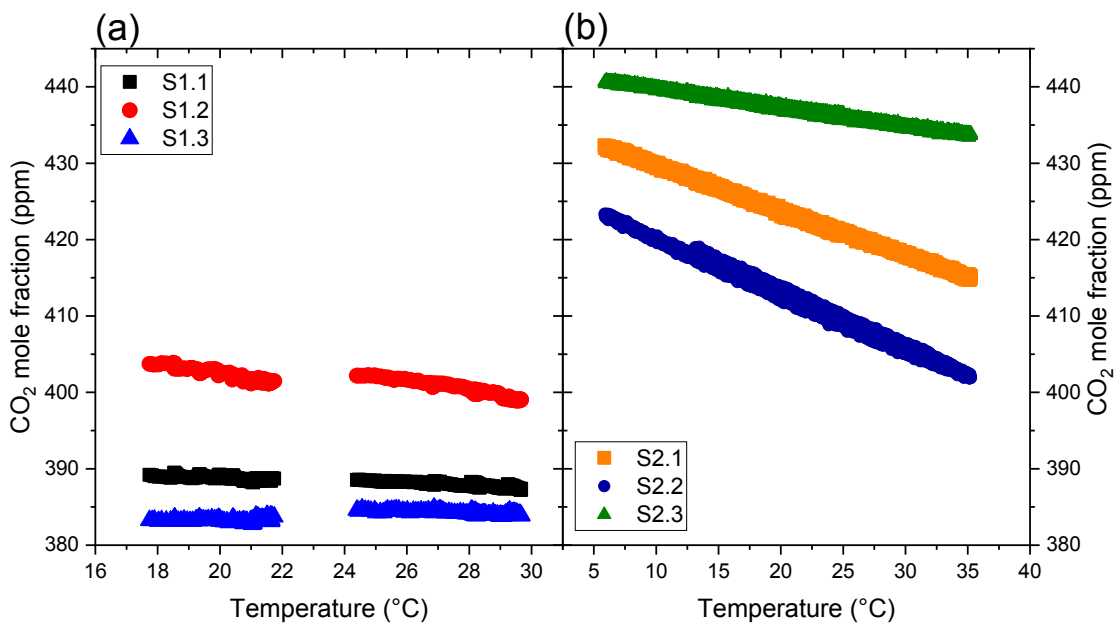
365

366 The PT2 tests results with pressure changes from 1013.25 to 759.94 hPa with an increment of
367 50.66 hPa are shown in Figure 4. The top panel of the Figure 4 shows the variations of CO₂ dry air
368 mole fractions due to p changes (from 0.0049 to 0.0177 ppm per hPa). Despite the built-in
369 pressure compensation algorithm developed for HPP3.2, reported {CO₂} and p can still co-vary
370 with a positive (S2.1 and S2.2) or a negative (S2.3) correlation, indicating that an additional
371 correction is required when aiming to achieve the best possible results (see also Figure S1.
372 Consequently, we applied a linear fit between $\Delta\{CO_2\}$ (differences between the assigned dry air
373 mole fraction in the cylinder and the dry air mole fraction reported by HPP3.2 instruments) and
374 pressure (Figure 6). The slope and intercept obtained are then used to determine the offset due
375 to p variations that has to be added on {CO₂} reported by the HPP3.2 instruments. The corrected
376 {CO₂} values have a root mean square deviation from the assigned dry air mole fraction in the
377 calibration cylinder (428.6 ppm) of less than 0.02 ppm for all three HPP3.2 (see also Figure S2).
378 Figure 5 shows the effect of temperature variations in the PIT chamber going from -2 to 35 °C
379 (see section 3.1) on reported CO₂ dry air mole fraction of the HPP3.2 instruments. For the three
380 HPP3.2, {CO₂} is negatively correlated to T. As for the tests in the simple chamber with the HPP3.1
381 instruments, different linear T slopes and intercepts are observed for each HPP3.1 instrument
382 (Figure 5) in the PIT chamber. After correction for temperature variations, we obtain corrected
383 {CO₂} values with a root mean square deviation which does not exceed 0.01 ppm from the
384 assigned value of the cylinder (444 ppm) for the three HPP3.2 instruments (see also Figure S3).



386
 387
 388
 389
 390

Figure 4: Linear relationship experimentally found between reported $\{CO_2\}$ and p for S1.1, S1.2, S1.3 (la) and for the instruments S2.1, S2.2, S2.3 (b). Note the different p range, going from 972.7 to 1030hPa for the HPP3.1 instruments in the simple plastic chamber and 759.9 to 1013.25hPa for the HPP3.2 instruments in the PIT chamber.



391
 392
 393
 394
 395

Figure 5: Linear relationships between reported $\{CO_2\}$ for S1.1 S1.1, S1.2 and S1.3 (la) at temperature values going from 17 to 30 °C in plastic chamber, and for S2.1, S2.2 and S2.3 at temperature values going from 5 to 35 °C in the PIT chamber (b).

396 Table 2 summarizes the results of the pressure and temperature tests for all instruments. These
 397 tests results show a sensor-specific response to p and T. A large difference of reported {CO₂}
 398 sensitivity to pressure variations is observed between the two HPP3 versions. A sensitivity of
 399 0.564 to 0.744 ppm/hPa is found for the HPP3.1 sensors, whereas this sensitivity ranges from -
 400 0.0045 up to 0.0174 ppm/hPa for the newer HPP3.2 sensors. The lower sensitivity among HPP3.2
 401 prototypes is due to the pressure compensation algorithm, which is included in this model. Since
 402 the pressure compensation algorithm does still not fully correct the reported {CO₂} variations due
 403 to pressure changes, we found that it is necessary to apply a correction for pressure, and that this
 404 correction should be sensor specific. The {CO₂} sensitivity to temperature variations are found to
 405 be in similar range for both sensor makes. Sensitivities of -0.3 to 0.1 ppm °C⁻¹ and -0.2 to -0.7
 406 ppm °C⁻¹ are found for HPP3.1 and HPP3.2 instruments, respectively.
 407

	Pressure			Temperature		
	Slope (ppm/hPa)	Intercept (ppm)	R ²	Slope (ppm/°C)	Intercept (ppm)	R ²
S1.1	0.664±0.004	-297.7 ±4.3	0.94	-0.124 ±0.003	391.34 ±0.07	0.85
S1.2	0.744 ±0.001	-363.3 ±1.1	0.95	-0.29 ±0.01	408.1 ±0.2	0.80
S1.3	0.564±0.001	-189.5 ±1.4	0.94	0.107 ±0.004	381.2 ±0.1	0.63
S2.1	0.0174 ±0.0002	394. ±0.2	0.95	-0.5854 ±0.0004	435.530 ±0.01	0.99
S2.2	0.0164 ±0.00001	392.4 ±0.2	0.97	-0.716 ±0.001	427.31 ±0.02	0.99
S2.3	-0.0045 ±0.0002	429.0 ±0.0	0.75	-0.2453 ±0.0004	442.16 ±0.01	0.99

408 **Table 2:** Slopes and intercept calculated for CO₂ correction due to temperature and pressure.
 409 Sensor S1.1 to S1.3 are type HPP3.1, whereas Sensor S2.1 to S2.3 are HPP3.2.
 410

411 After applying our correction for temperature and pressure, no more correlations are observed
 412 between corrected {CO₂} and pressure and temperature. Corrected CO₂ mole fractions of HPP3.2
 413 are stable and standard errors do not exceed 0.3 ppm and 0.2 ppm for pressure and temperature
 414 corrections respectively, except for {CO₂} after temperature correction for S2.2 which reaches a
 415 standard deviation (STD) of 0.5 ppm. However, we do not reach the same stability after pressure
 416 and temperature correction for HPP3.1 prototypes. Standard deviations of 0.9, 0.2 and 0.2 ppm
 417 are calculated for S1.1, S1.2 and S1.3 respectively after pressure correction, and Standard
 418 deviations of 1.3, 2.6 and 1.6 ppm are determined for S1.1, S1.2 and S1.3 respectively after
 419 temperature corrections. These differences between the results of the two HPP3 versions can be
 420 partly explained by the fact that HPP3.2 prototypes had the opportunity to be tested in a
 421 sophisticated climatic chamber which respects precise temperature and pressure set points for

422 more longer-term measurements and in which only one of the two variables are modified one at a
423 time.

424

425 4.2. Instrument calibration and stability during continuous measurements

426

427 Our instrument described in this study is intended for use in field campaign studies and longer-
428 term monitoring, we assess their performance during continuous measurements. We also
429 evaluate which calibration frequency is necessary to track the changes in the sensitivities to p and
430 T found in section 4.1 and if the instruments can be calibrated when using an undried gas stream.
431 Given that the instrument response to $\{CO_2\}$ is also affected by atmospheric water vapor, we
432 present the results from dried and wet ambient air measurements separately.

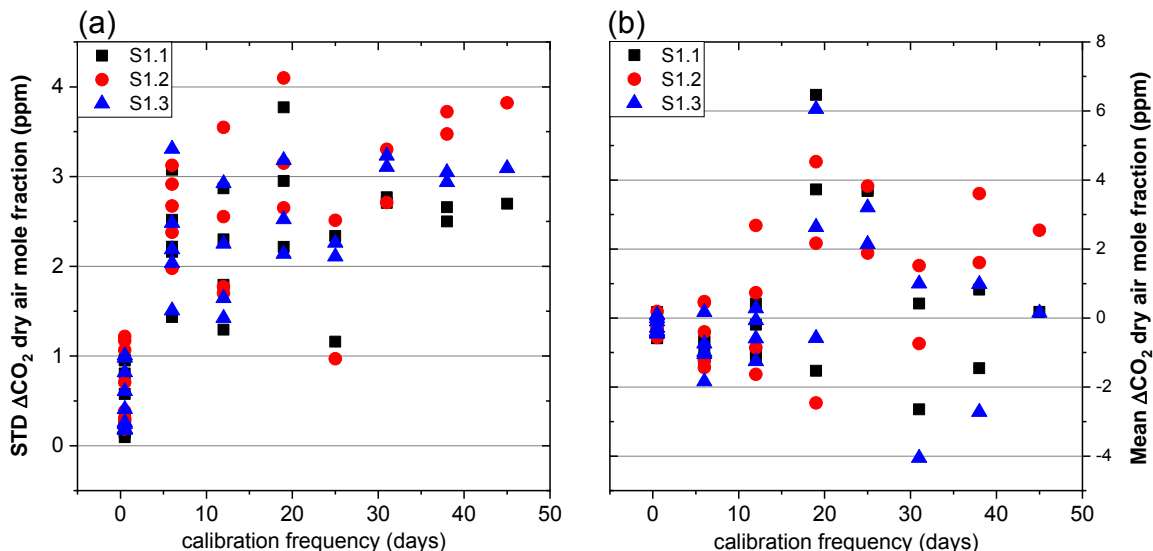
433

434 4.2.1. Measurements of dried ambient air (DA1)

435

436 Four calibration cylinders were used in order to calibrate the three HPP3.1 instruments (see
437 section 3.1). To assess the quality of this calibration, the mean and standard deviation (STD) of
438 $\Delta\{CO_2\}$ (i.e. $\{CO_2\}_{HPP3} - \{CO_2\}_{CRDS}$) of 1-minute averaged data were calculated, and shown in Figure
439 6. Although calibration cylinders were measured each 12 hours, by ignoring some calibration data,
440 we processed the time series to re-compute calibrated $\{CO_2\}$ assuming a range of different time
441 intervals between two calibrations. The results shown in Figure 6 are for calibrations intervals of
442 0.5, 6, 12, 19, 25, 31, 38 and 45 days. Each point in this Figure corresponds to the values
443 calculated for the instruments S1.1, S1.2, S1.3.

444 We find that the 1 ppm repeatability threshold is nearly met when measuring dried air for calibration
445 intervals of 6 days. The STD $\Delta\{CO_2\}$ of the minute averages slowly increases with increasing
446 calibration intervals but seems to stabilize between 3 and 4 ppm. We also see a marked difference
447 between the performances of each sensor: S1.1 shows the best performance, followed by S1.3
448 and S1.2. Besides an increased STD, we also see that the mean of $\Delta\{CO_2\}$ increases significantly
449 after not calibrating for 19 days. Surprisingly, one calibration each 45 days does not seem to
450 deteriorate the mean of $\Delta\{CO_2\}$ further. Infact, the mean $\Delta\{CO_2\}$ seems to decrease over longer
451 time periods.



452

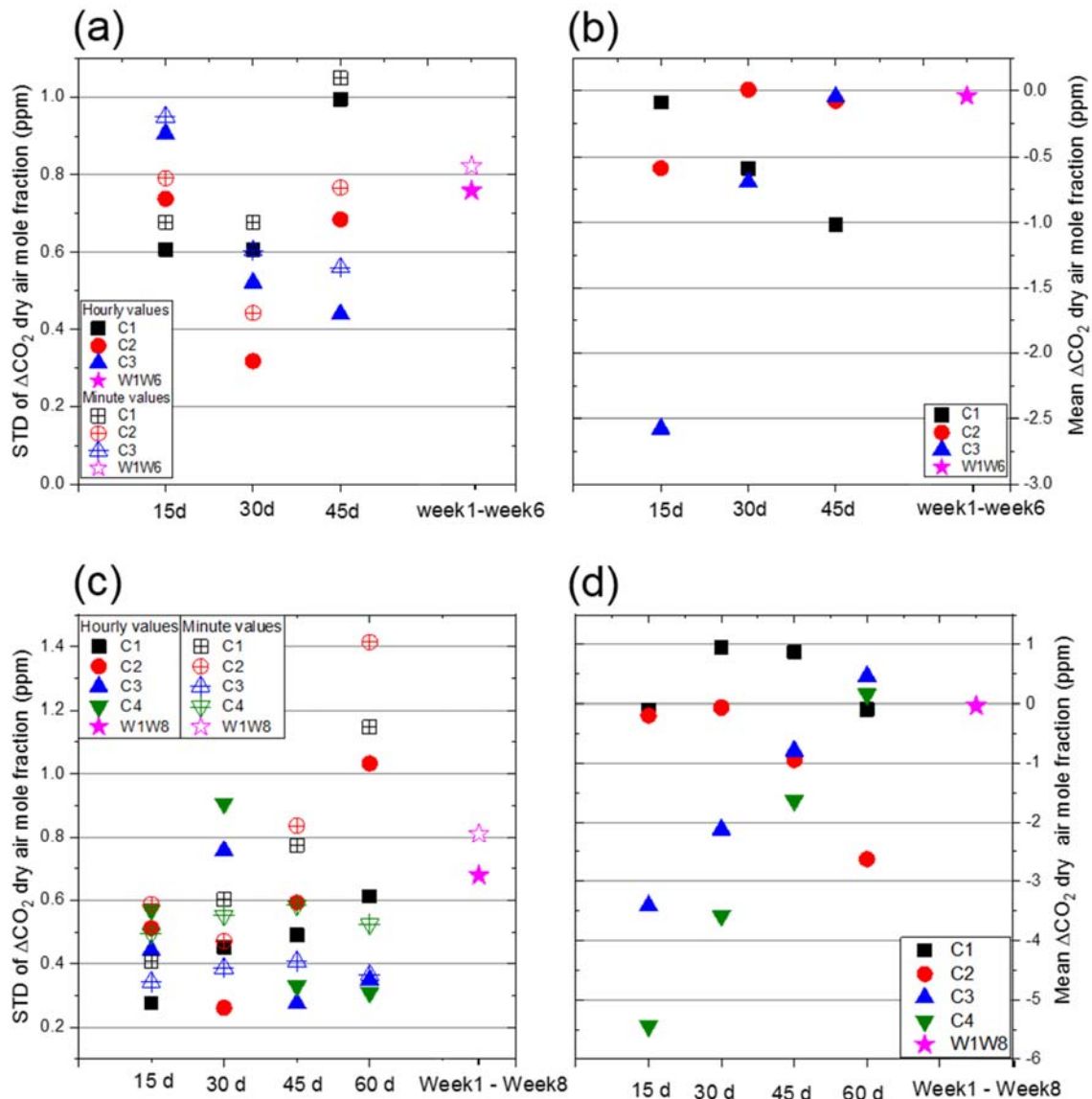
453 **Figure 6:** STD (a) and mean (b) values of one minute average of mean $\Delta\{CO_2\}$, during a
454 measurement period of 48 days depending of the calibration frequency.

455

456 **4.2.2. Saclay ambient air measurements (WA2-1)**

457
458 During this test (section 3.3.1), $\{CO_2\}$ and variables affecting the instrument stability, i.e. pressure,
459 temperature, water vapor content and were measured from July 20th until August 8th. The
460 meteorological parameters during the field campaign are given in Figure S4. Our previous
461 measurements already indicated that regular recalibration of the HPP3s is required because of
462 sensitivities to T, p and water vapor that are instrument-specific and time dependent. We call the
463 period during which the six calibration coefficients of Eq. (1) are calculated by using the CRDS
464 $\{CO_2\}$ time series, the calibration period. Attempting to determine those calibration coefficients
465 during a short calibration period e.g. of one week, leads to high mean $\Delta\{CO_2\}$, as can be seen in
466 Figure 7. A calibration period of two weeks leads to significantly better results. We benchmark the
467 instrument performance for both minute averages, the instruments typical temporal resolution, and
468 hourly averages, as those are widely used in modelling studies and data assimilation systems.
469 We also compared different calibration periods of the same length. As an example, considering a
470 45 days experiment, we chose three different calibration periods of successive 15 days. We also
471 tested the approach of using the first and last weeks of a 45 days period to create a non-
472 successive two weeks calibration period.

473 Figure 7 (a,b) shows the STD and mean $\Delta\{CO_2\}$ values considering 3 calibration periods (C1, C2,
474 C3) of 15 days each. The regression coefficients of the multivariable model of Eq. (1) for C1, C2
475 and C3 are calculated using the first, second and third consecutive 15 days of the experimental
476 period. These coefficients are then used to predict corrected $\{CO_2\}_{HPP3}$ for the three cross-
477 validation periods of 15, 30 and 45 days. Also, calibration coefficients (W1, W6) were calculated
478 using the first and sixth week of the 45 days period for calibration. Unsurprisingly, using C1
479 coefficients gives the best results for the first 15 days used for training, and lead a higher bias for
480 the last 15 days. Using C2 coefficients to correct adjacent 15 days from the calibration period
481 gives comparable results. Considering the last calibration period, C3 coefficients show a mean
482 bias of -2.5 ppm when calibration is from the first 15 days. One reason that can explain this
483 behavior is the greater variability of CO_2 dry air mole fraction during the last 15 days of the
484 experiment. The interquartile range of CO_2 dry air mole fraction is 10, 15 and 25 ppm respectively
485 for the first, second and third period. The CO_2 dry air mole fraction correction is accomplished
486 mostly by correcting T, P, H_2O and the instrument offset. A small variation of sensitivities may lead
487 to a less appropriate correction for periods of smaller variability. Another reason for this difference
488 is the drift component of the correction in Eq. 1. The linear drift of the instrument also varies with
489 time. One method to better correct for the slow linear drift of the instrument is to combine the first
490 and last week of the experiment into a calibration period instead of using two consecutive weeks.
491 When using the first week (W1) and the last week (W6) for calibration, the instrument drift is not
492 properly corrected and a residual linear drift of 0.14 and 0.28 ppm/week is visible in the black (W1)
493 and the red (W6) curves of Figure S5, respectively. Nearly no drift (0.01 ppm/week) is observed
494 when considering both W1 and W6 for the training (blue curve). On Figure 7, magenta stars show
495 STD $\Delta\{CO_2\}$ and mean $\Delta\{CO_2\}$ values of the whole 45 day time series considering both W1 and
496 W6 as calibration periods. With this coefficient determination method, mean ΔCO_2 bias can be
497 reduced to nearly 0 ppm. Finally, we should note that averaging the 1-minute data to hourly
498 averages can further improve STD $\Delta\{CO_2\}$ values up to 28%. As expected, mean values do not
499 change for hourly averages.



500
 501 **Figure 7:** STD $\Delta\{CO_2\}$ (a) and mean $\Delta\{CO_2\}$ (b) values considering 3 calibration periods of 15
 502 consecutive days for calibration each with C1, C2 and C3 correspond to first, second and third
 503 consecutive days of measurements at the Saclay field site, respectively. W1W6 corresponds to
 504 using the first and sixth week as calibration period. Mean ΔCO_2 calculated for the four calibration
 505 periods choices. STD $\Delta\{CO_2\}$ (c) and mean $\Delta\{CO_2\}$ (d) values considering 4 calibration periods of
 506 15 consecutive days for calibration each with C1, C2, C3, C4 correspond to first, second, third and
 507 fourth 15 consecutive days of measurements at the Jussieu field site, respectively. W1W6
 508 corresponds to using the first and eight week as calibration period. Hourly and minute values are
 509 represented in full and empty symbols respectively.

510 Furthermore, we can investigate which of the six term multivariable linear regression is most
 511 important here. The offset and dry air mole fraction dependent corrections terms (b and
 512 $a_{CO_2}\{CO_2\}_{HPP3}$) are the most significant corrections among all 5 parameters and allow reducing the

513 mean ΔCO_2 from 45 ppm to 0 ppm (see Table 3 and Figure S3). The other 4 parameters (pressure,
 514 temperature, water vapor and drift corrections) further reduce the difference between CRDS and
 515 HPP3.2 reducing the STD $\Delta\{\text{CO}_2\}$ of minute averages from 1.03 ppm to 0.67 ppm. Here, the
 516 temperature correction (d) and the water vapor correction (e) provide a correction of similar
 517 magnitude, keeping the same STD and improving mean $\Delta\{\text{CO}_2\}$ only from 0.16 to 0.13 ppm. This
 518 is understandable since temperature and water vapor are correlated for this type of measurement.
 519

	Reported (raw)	Offset correction	Pressure correction	Temperature correction	RH correction	Drift correction
STD $\Delta\{\text{CO}_2\}$ (ppm)	1.11	1.03	1.00	0.97	0.97	0.67
Mean $\Delta\{\text{CO}_2\}$ (ppm)	45.33	$1 \cdot 10^{-3}$	$9 \cdot 10^{-4}$	0.16	0.13	-0.08

520 **Table 3:** STD and mean values of one minute average $\Delta\{\text{CO}_2\}$ data for each correction step. Note
 521 that corrections are cumulative from left to right.
 522

523 **4.2.3. Jussieu ambient air measurements (WA2-2)**

524
 525 To assess the further performance of the HPP3.2 instruments, additional wet ambient air
 526 measurements at second field site in Jussieu were carried out for 60 consecutive days using
 527 instrument S2.1 alongside a CRDS. Figure 7 (c,d) shows STD $\Delta\{\text{CO}_2\}$ and mean $\Delta\{\text{CO}_2\}$ values
 528 calculated with four calibration periods of 15 consecutive days each and one calibration
 529 considering both first and last week of the experiment. Calibration coefficients for C1, C2, C3 and
 530 C4 are calculated considering calibration periods of first, second, third and fourth 15 consecutive
 531 days of the experiment respectively. W1W8 coefficients are calculated considering week one (W1)
 532 and week eight (W8) of the experiment. The results are qualitatively very similar to the
 533 measurements at the Saclay field site and combining the first and last week as calibration period
 534 also results allow achieving our target of STD $\Delta\{\text{CO}_2\} > 1\text{ppm}$.
 535

536 **5. Conclusion and perspective**

537
 538 We integrated HPP3.1 and HPP3.2 NDIR sensors into a portable low-cost instrument with
 539 additional sensors and internal data acquisition. The laboratory tests reveal a strong sensitivity of
 540 reported CO_2 dry air mole fractions to ambient air pressure for the HPP3.1 series and a
 541 significantly decreased, yet noticeable, sensitivity to pressure, for the upgraded HPP3.2 sensors
 542 equipped with the built-in manufacturer p-correction. To achieve the targeted stability (long-term
 543 repeatability) for urban observations of 1 ppm or better, instruments have to be corrected at regular
 544 intervals against data from a reference instrument (here: CRDS) to account for their cross-
 545 sensitivities to T , p , W (H_2O mixing ratio) changes and electronic drift, unless those parameters
 546 could be controlled externally in the future. We found that commercially available p , T and RH
 547 sensors that are compatible with the chosen Raspberry Pi3 platform are sufficiently precise to use
 548 these parameters as predictors of the linear equation use to calibrate each HPP3 instrument
 549 against the reference instrument, which was calibrated to the official WMO CO_2 X2007 CO_2 scale.

550 Two common modes of operation have been successfully tested i.e. using the HPP3 instruments
551 for either dried or undried ambient air measurements. Our results indicate that using a dried gas
552 stream does not improve measurement precision or stability compared to an undried gas streams
553 provided that a multivariable regression model is used for calibration, which accounts for all cross-
554 sensitivities including to H₂O mixing ratio changes.

555 We furthermore find that sensor specific corrections are required and they should be considered
556 time-dependent, e.g. by including a linear drift that only becomes more apparent for longer-term
557 observations. Different calibration windows were tested for both the Saclay field site and Jussieu
558 field site ambient air measurements and their results evaluated against CRDS data that were not
559 used for calibration. Those sites exhibit the typical {CO₂} levels in urban GHG monitoring networks
560 where future low-cost medium precision instruments could be deployed. Regular (six weekly) re-
561 calibrations are found to be appropriate to capture sensor drifts and changes in relevant cross-
562 sensitivities, while not increasing the burden of performing calibration too often. A dedicated set
563 of calibration gases was not necessary if the low cost instrument was calibrated against {CO₂}
564 from a CRDS using the same air. Calibration periods of one week with parallel CRDS
565 measurements before and after a 45 day deployment was sufficient for the STD Δ{CO₂} data to
566 be within 1 ppm of CRDS during that period (with near zero bias, i.e. Δ{CO₂} << 1 ppm) . This
567 calibration approach can thus be an alternative to permanently deploying calibration gases for
568 each individual sensor..

569 The field tests at the Saclay and Jussieu station are being continued to see if the instrument
570 performance deteriorates over its lifetime. Since the start of the test in 2015 until now multiple
571 HPP3.1 sensors have been in use for without significant performance loss. Other research groups
572 have also started integrating HPP sensors into their low-cost GHG monitoring strategy (e.g.
573 Carbosense, www.nano-tera.ch/projects/491.php, last access March 11th, 2019).

574 Future improvements for the LCMP instruments will include the addition of batteries to allow their
575 transport to the central calibration lab without power cut as well as using them in field campaigns,
576 e.g. landfills when connected to solar panels or small wind turbines. During future tests at sites
577 without reference instruments, small pressurized gas containers (12l, minican, Linde Gas) will be
578 used to regularly inject target gas to track the performance during a deployment period.

579 The overall operational cost of the new calibration scheme using a central laboratory and rotating
580 the LCMP systems can also only be assessed after more extensive field deployment has been
581 performed.

582

583 **Code and data availability**

584 The python scripts for the data collection from the HPP3 and DHT22 for Raspberry Pi-3 and the
585 data from the experiments described here are available from the corresponding authors upon
586 request.

587

588 **Author contributions**

589 The shared first authors EA and FRV conducted the measurements reported in this study and
590 planned the work with support of PC. AB and BG supported the development of the data logging
591 routine and processing scripts. OL and MR supported measurements by providing access to the
592 ICOS test laboratory equipment and supplied reference gases. The initial draft of the manuscript
593 was developed by EA, FRV and PC. All authors have updated, contributed and edited the
594 manuscript.

595

596 **Acknowledgements**

597 The work conducted here was partially funded through the LOCATION project of the Low Carbon
598 City Laboratory and a SME-VOUCHER from climate-KIC (EIT) as well as the Chaire BridGES of
599 UVSQ, CEA, Thales Alenia Space and Veolia S.A.

600

601 **References**

602

603 Andres, R. J., Boden, T. A., and Higdon, D.: A new evaluation of the uncertainty associated with
604 CDIAC estimates of fossil fuel carbon dioxide emission, *Tellus B*, 66, 23616,
605 doi:10.3402/tellusb.v66.23616, 2014.

606

607 Bréon, F. M., Broquet, G., Puygrenier, V., Chevallier, F., Xueref-Remy, I., Ramonet, M.,
608 Dieudonné, E., Lopez, M., Schmidt, M., Perrussel, O., and Ciais, P.: An attempt at estimating Paris
609 area CO₂ emissions from atmospheric concentration measurements, *Atmos. Chem. Phys.*, 15,
610 1707-1724, <https://doi.org/10.5194/acp-15-1707-2015>, 2015.

611

612 Broquet, G., Bréon, F.-M., Renault, E., Buchwitz, M., Reuter, M., Bovensmann, H., Chevallier, F.,
613 Wu, L., and Ciais, P.: The potential of satellite spectro-imagery for monitoring CO₂ emissions from
614 large cities, *Atmos. Meas. Tech. Discuss.*, <https://doi.org/10.5194/amt-2017-80>, in review, 2017.

615

616 Cambaliza, M. O. L., Shepson, P. B., Caulton, D. R., Stirm, B., Samarov, D., Gurney, K. R.,
617 Turnbull, J., Davis, K. J., Possolo, A., Karion, A., Sweeney, C., Moser, B., Hendricks, A., Lauvaux,
618 T., Mays, K., Whetstone, J., Huang, J., Razlivanov, I., Miles, N. L., and Richardson, S. J.:
619 Assessment of uncertainties of an aircraft-based mass balance approach for quantifying urban
620 greenhouse gas emissions, *Atmos. Chem. Phys.*, 14, 9029-9050, [https://doi.org/10.5194/acp-14-](https://doi.org/10.5194/acp-14-9029-2014)
621 9029-2014, 2014.

622

623 Eugster, W. and Kling, G. W.: Performance of a low-cost methane sensor for ambient
624 concentration measurements in preliminary studies, *Atmos. Meas. Tech.*, 5, 1925–
625 1934, <https://doi.org/10.5194/amt-5-1925-2012>, 2012.

626

627 GAW report 242,: 19th WMO/IAEA Meeting on Carbon Dioxide, Other Greenhouse Gases and
628 Related Measurement Techniques (GGMT-2017), World Meteorological Organization, edited by
629 Crotwell, A. and Steinbacher M., 2018, available at:

630 https://library.wmo.int/doc_num.php?explnum_id=5456, last access Feb. 10th, 2018

631

632 Gaynullin, B., Bryzgalov, M., Hummelgård C., and Rödjegård, H., "A practical solution for accurate
633 studies of NDIR gas sensor pressure dependence. Lab test bench, software and calculation
634 algorithm," 2016 *IEEE SENSORS*, Orlando, FL, 2016, pp. 1-3. Doi:
635 10.1109/ICSENS.2016.7808828.

636

637 Holstius, D. M., Pillarisetti, A., Smith, K. R., & Seto, E. (2014). Field calibrations of a low-cost
638 aerosol sensor at a regulatory monitoring site in California. *Atmospheric Measurement*
639 *Techniques*, 7(4), 1121-1131, <https://doi.org/10.5194/amt-7-1121-2014>, 2014.

640

641 Hummelgård, C., Bryntse, I., Bryzgalov, M., Henning, J.-Å., Martin, H., Norén, M., and Rödjegård,
642 H.: Low-Cost NDIR Based Sensor Platform for Sub-Ppm Gas Detection, *Urban Climate*, 14, Part
643 3, 342–350, doi:10.1016/j.uclim.2014.09.001, 2015.

644

645 Kunz, M., Lavric, J. V., Gerbig, C., Tans, P., Neff, D., Hummelgård, C., Martin, H., Rödjegård, H.,
646 Wrenger, B., and Heimann, M.: COCAP: a carbon dioxide analyser for small unmanned aircraft
647 systems, *Atmos. Meas. Tech.*, 11, 1833-1849, <https://doi.org/10.5194/amt-11-1833-2018>, 2018.

648
649 Lauvaux, T., et al. (2016), High-resolution atmospheric inversion of urban CO₂ emissions during
650 the dormant season of the Indianapolis Flux Experiment (INFLUX), *J. Geophys. Res. Atmos.*, 121,
651 5213–5236, doi:10.1002/2015JD024473.
652
653 Liu, Z., He, C., Zhou, Y., and Wu, J.: How much of the world's land has been urbanized, really?
654 A hierarchical framework for avoiding confusion, *Landscape Ecol.*, 29, 763–771,
655 doi:10.1007/s10980-014-0034-y, 2014.
656
657 Martin, C. R., Zeng, N., Karion, A., Dickerson, R. R., Ren, X., Turpie, B. N., and Weber, K. J.:
658 Evaluation and environmental correction of ambient CO₂ measurements from a low-cost NDIR
659 sensor, *Atmos. Meas. Tech.*, 10, 2383-2395, <https://doi.org/10.5194/amt-10-2383-2017>, 2017.
660
661 Mays, K. L., Shepson, P. B., Stirm, B. H., Karion, A., Sweeney, C., & Gurney, K. R. (2009).
662 Aircraft-based measurements of the carbon footprint of Indianapolis. *Environmental Science and*
663 *Technology*, 43(20), 7816-7823. DOI: 10.1021/es901326b.
664
665 Nassar, R., Hill, T. G., McLinden, C. A., Wunch, D., Jones, D. B. A., & Crisp, D. (2017). Quantifying
666 CO₂ emissions from individual power plants from space. *Geophysical Research Letters*, 44,
667 10,045–10,053. <https://doi.org/10.1002/2017GL074702>.
668
669 Piedrahita, R., Xiang, Y., Masson, N., Ortega, J., Collier, A., Jiang, Y., Li, K., Dick, R. P., Lv, Q.,
670 Hannigan, M., and Shang, L.: The next generation of low-cost personal air quality sensors for
671 quantitative exposure monitoring, *Atmos. Meas. Tech.*, 7, 3325–3336,
672 <https://doi.org/10.5194/amt-7-3325-2014>, 2014.
673
674 Raspberry Pi Foundation: Raspberry Pi Hardware Documentation, available at:
675 <https://www.raspberrypi.org/documentation/hardware/raspberrypi/>
676
677 Rella, C. W., Chen, H., Andrews, A. E., Filges, A., Gerbig, C., Hatakka, J., Karion, A., Miles, N. L.,
678 Richardson, S. J., Stein-bacher, M., Sweeney, C., Wastine, B., and Zellweger, C.: High accuracy
679 measurements of dry mole fractions of carbon dioxide and methane in humid air, *Atmos. Meas.*
680 *Tech.*, 6, 837–860, doi:10.5194/amt-6-837-2013, 2013.
681
682 Shusterman, A. A., Teige, V. E., Turner, A. J., Newman, C., Kim, J., and Cohen, R. C. (2016). The
683 BErkeley atmospheric CO₂ observation network: initial evaluation. *Atmospheric Chemistry and*
684 *Physics*, 16(21), 13449-13463.
685
686 Seto, K. C., Dhakal, S., Bigio, A., Blanco, H., Delgado, G. C., Dewar, D., Huang, L., Inaba, A.,
687 Kansal, A., Lwasa, S., McMahon, J. E., Müller, D. B., Murakami, J., Nagendra, H., and
688 Ramaswami, A.: Human settlements, infrastructure and spatial planning, in: *Climate Change*
689 *2014: Mitigation of Climate Change. Contribution of Working Group III to the Fifth Assess-*
690 *ment Report of the Intergovernmental Panel on Climate Change*, edited by: Edenhofer, O.,
691 Pichs-Madruga, R., Sokona, Y., Farahani, E., Kadner, S., Seyboth, K., Adler, A., Baum, I., Brun-
692 ner, S., Eickemeier, P., Kriemann, B., Savolainen, J., Schlömer, S., von Stechow, C., Zwickel,
693 T., and Minx, J. C., Cambridge, United Kingdom and New York, NY, USA, 2014.
694
695 Stauffer, J., Broquet, G., Bréon, F.-M., Puygrenier, V., Chevallier, F., Xueref-Rémy, I., Dieudonné,
696 E., Lopez, M., Schmidt, M., Ramonet, M., Perrussel, O., Lac, C., Wu, L., and Ciais, P.: The first 1-
697 year-long estimate of the Paris region fossil fuel CO₂ emissions based on atmospheric inversion,
698 *Atmos. Chem. Phys.*, 16, 14703-14726, <https://doi.org/10.5194/acp-16-14703-2016>, 2016.

699
700 Turner, A. J., Shusterman, A. A., McDonald, B. C., Teige, V., Harley, R. A., and Cohen, R. C.:
701 Network design for quantifying urban CO₂ emissions: assessing trade-offs between precision
702 and network density, *Atmos. Chem. Phys.*, 16, 134650013475, [https://doi.org/10.5194/acp-16-](https://doi.org/10.5194/acp-16-13465-2016)
703 13465-2016, 2016.
704
705 Verhulst, K. R., Karion, A., Kim, J., Salameh, P. K., Keeling, R. F., Newman, S., Miller, J., Sloop,
706 C., Pongetti, T., Rao, P., Wong, C., Hopkins, F. M., Yadav, V., Weiss, R. F., Duren, R. M., and
707 Miller, C. E.: Carbon dioxide and methane measurements from the Los Angeles Megacity Carbon
708 Project – Part 1: calibration, urban enhancements, and uncertainty estimates, *Atmos. Chem.*
709 *Phys.*, 17, 8313-8341, <https://doi.org/10.5194/acp-17-8313-2017>, 2017.
710
711 Wang, Y., Li, J. Y., Jing, H., Zhang, Q., Jiang, J. K., and Biswas, P.: Laboratory Evaluation and
712 Calibration of Three Low- Cost Particle Sensors for Particulate Matter Measurement, *Aerosol Sci.*
713 *Tech.*, 49, 1063–1077, <https://doi.org/10.1080/02786826.2015.1100710>, 2015.
714
715 Wu, L., Broquet, G., Ciais, P., Bellassen, V., Vogel, F., Chevallier, F., Xueref-Remy, I., and Wang,
716 Y.: What would dense atmospheric observation networks bring to the quantification
717 of city CO₂ emissions?, *Atmos. Chem. Phys.*, 16, 7743–7771, [https://doi.org/10.5194/acp-16-](https://doi.org/10.5194/acp-16-7743-2016)
718 7743-2016, 2016.
719
720 Young, D. T., Chapman, L., Muller, C. L., Cai, X. M., and Grimmond, C. S. B.: A Low-Cost Wireless
721 Temperature Sensor: Evaluation for Use in Environmental Monitoring Applications, *J. Atmos.*
722 *Ocean. Tech.*, 31, 938–944, <https://doi.org/10.1175/jtech-d-13-00217.1>, 2014.
723
724 Yver Kwok, C., Laurent, O., Guemri, A., Philippon, C., Wastine, B., Rella, C. W., Vuillemin, C.,
725 Troung, F., Delmotte, M., Kazan, V., Dardin, M., Lebegue, B., Kaiser, C., Xueref-Remy, I., and
726 Ramonet, M., Comprehensive laboratory and field testing of cavity ring-down spectroscopy
727 analyzers measuring H₂O, CO₂, CH₄ and CO. *Atmospheric Measurement Techniques*, 8(9),
728 3867-3892, 2015
729
730 Zimmerman, N., Presto, A.A., Kumar, S.P.N., Gu, J., Hauryliuk, A., Robinson, E.S., Robinson,
731 A.L., Subramanian, R., A machine calibration calibration model using random forests to improve
732 sensor performance for lower-cost air quality monitoring. *Atmos. Meas. Tech.* 11, 291-313.,
733 2018.